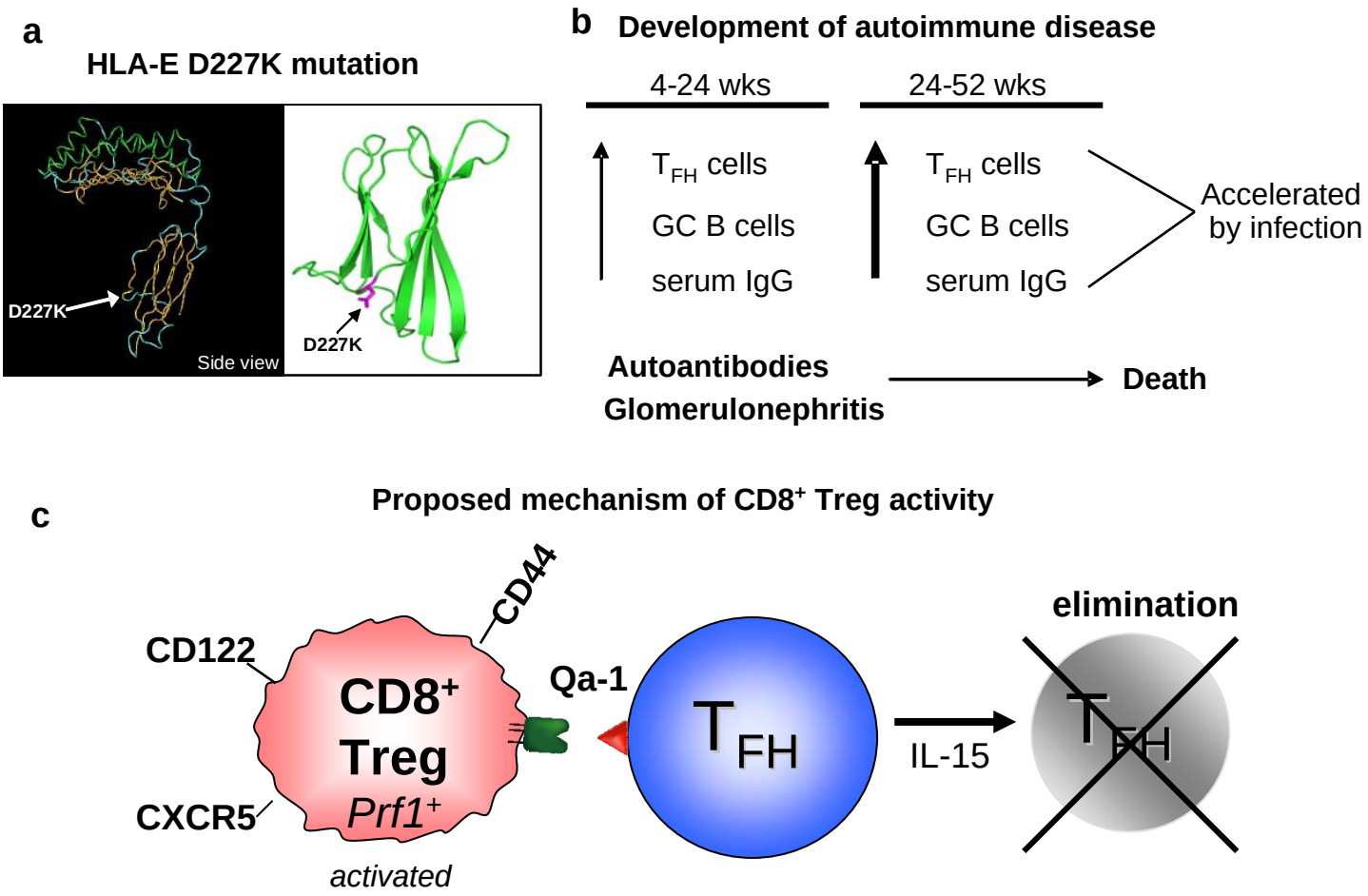

Supplementary Figure 1. **a**) **Three dimensional structure of HLA-E** and the position of the mutation that results in disruption of CD8 binding to HLA-E (or Qa-1) molecule. B6-Qa-1(D227K) knock-in mice were generated by mutating the amino acid position of 227 in CD8 binding alpha 3 domain of Qa-1 molecule from aspartic acid (**D**) to lysine (**K**). Expression of cell surface Qa-1 by activated CD4 cells from B6-Qa-1(D227K) knock-in mice was indistinguishable from B6-(Qa-1WT) mice [9]. Expression of the B6-Qa-1(D227K) mutation by L cells or activated CD4 cells failed to target these cells for lysis by Qa-1-restricted cytolytic T cells, while Qa-1/Qdm-dependent resistance of activated B6-Qa-1(D227K) CD4 cells to lysis by NKG2A$^+$ NK cells was unimpaired in vitro and in vivo [9].

b) **Development of autoimmune disease in Qa-1 D227K mice.** The Qa-1 mutation delineated in **a** develop the autoimmune disease characterized by tissue-specific autoantibodies, invasion of non-lymphoid tissues by monocytes/ lymphocytes and lethal glomerulonephritis. This disorder is associated with enhanced numbers of T_{FH} cells, activated lymphoid follicles, increased GC B cells, and is accelerated by viral infection.

c) Proposed mechanism of CD8$^+$ Treg activity. Activation of follicular helper T cells stimulates a subpopulation of Qa-1-restricted CD8$^+$ T cells that express the indicated surface molecules. These cells, termed CD8$^+$ Treg, may mediate perforin/ IL-15 dependent elimination of target Qa-1$^+$ T_{FH}.

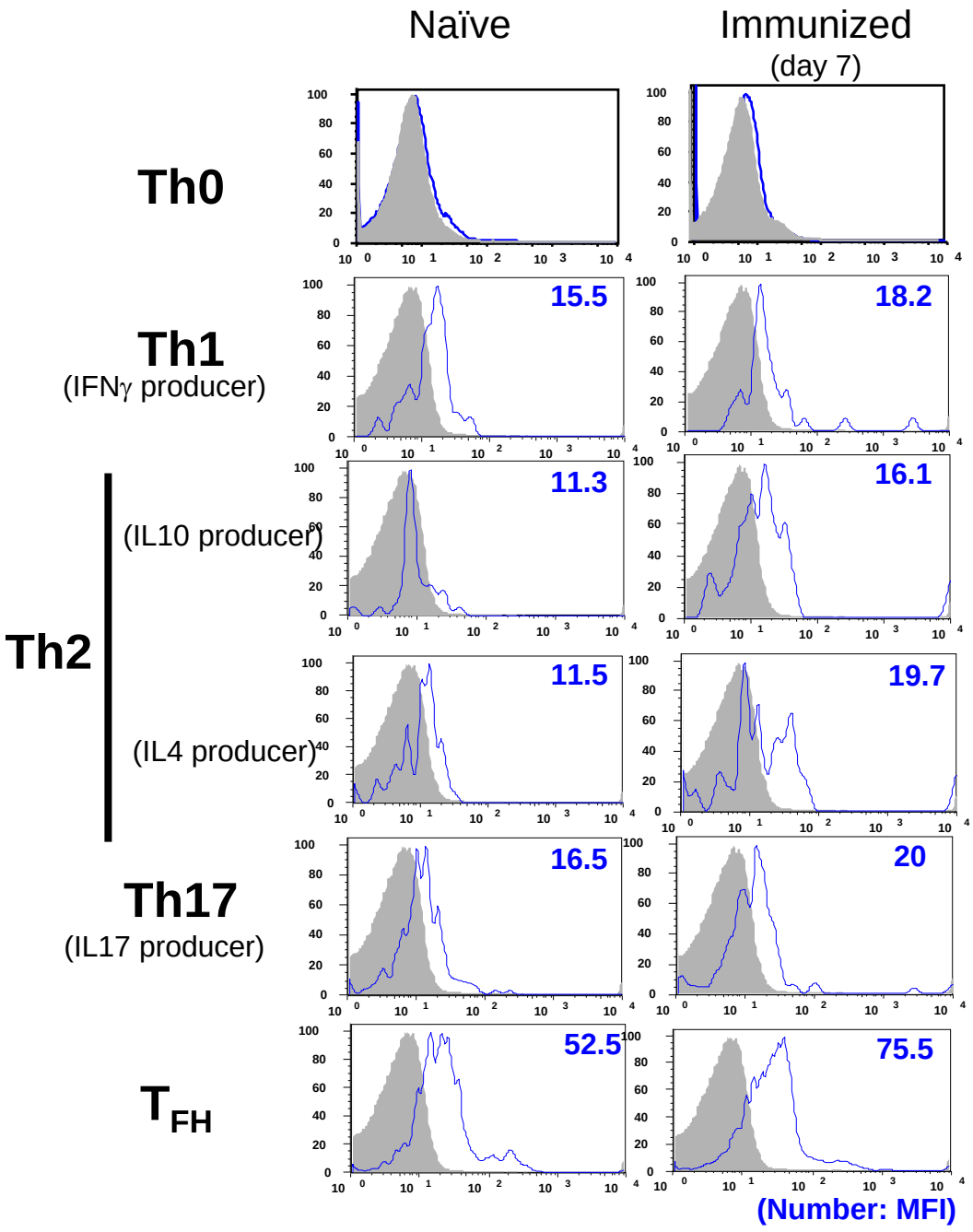

Supplementary Figure 2. **Qa-1 expression by Th cell lineages**.

Spleen cells from 6 week old naïve and KLH/CFA-immunized mice were analyzed for Qa-1 expression on cell surface. IFNγ^{+}IL-4^{-} cells were defined as Th1 cells; IL-10 or IL-4 producers were defined as Th2 cells; IL-17 producers were defined as Th17 cells. T_{FH} cells were identified by ICOS and B200 expression. Numbers shown represent mean fluorescence intensity (MFI).

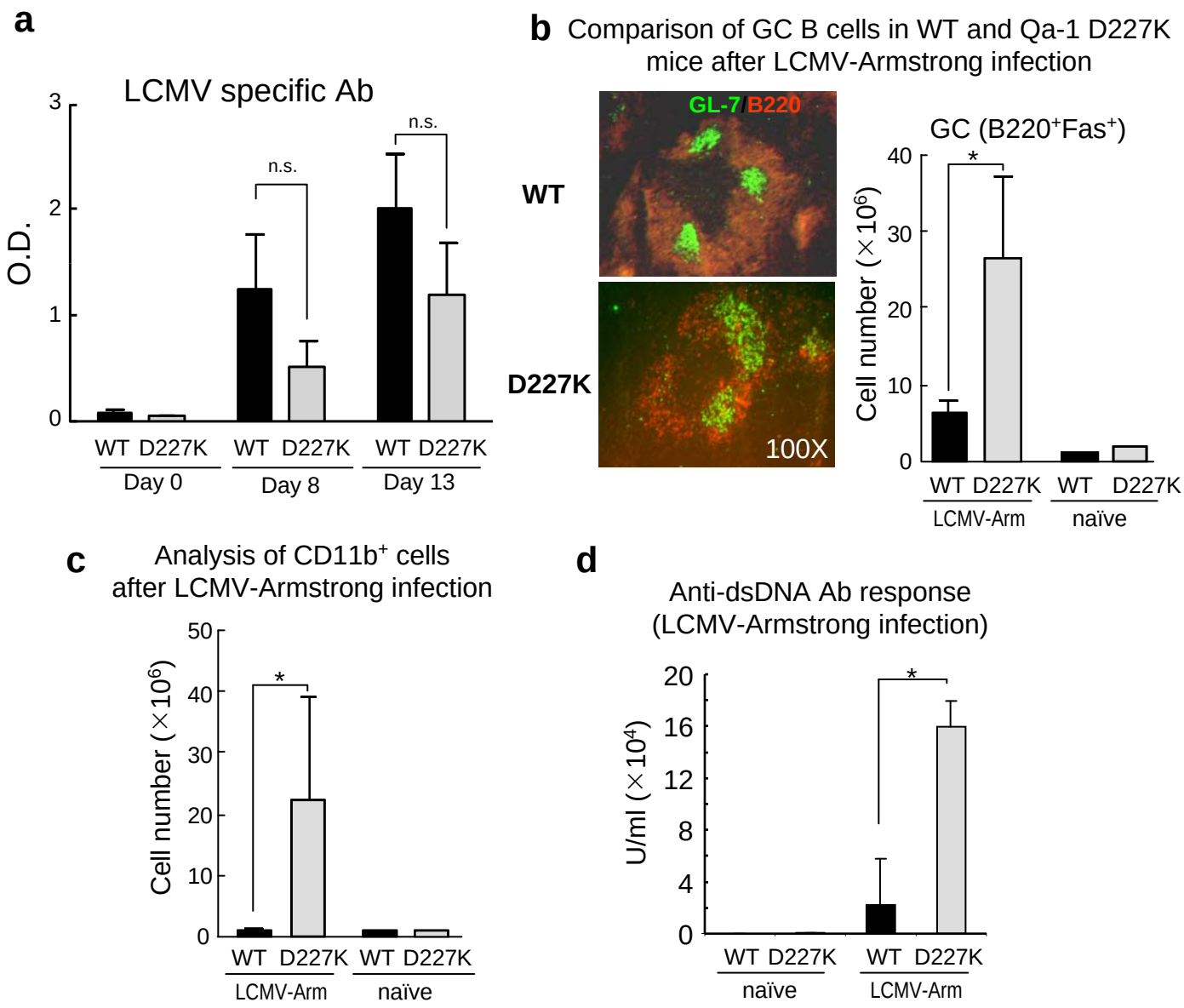

Supplementary Figure 3. Immune response of B6-(Qa-1^{WT}) and B6-Qa-1(D227K) mice upon LCMV-Armstrong infection. 6m old WT B6 and B6-Qa-1(D227K) mice were infected i.p. with 10^6 PFU LCMV-Armstrong. At day 8, mice were reinfected i.p. with 10^5 PFU LCMV-Armstrong. At days 8 and 13, sera from naïve and LCMV-Armstrong-infected WT and B6-Qa-1(D227K) mice were analyzed for the production of LCMV specific antibodies (**a**). **b and c**) Splenocytes from naïve or LCMV-Armstrong infected WT or B6-Qa-1(D227K) mice were analyzed for immune cell composition. Spleens from LCMV-Armstrong infected WT or B6-Qa-1(D227K) mice were analyzed for GC formation by immunohistochemistry (**b**, left panel)**.** Shown are representative B cell follicles stained for B220$^+$ cells (red) and GC B cells (GL-7$^+$, green). Increased size of GC and loose distribution of GL-7$^+$ cells in B6-Qa-1(D227K) mice suggest robust B cell activation and advanced stage of GC reaction characterized by light zone dominant GC phenotype. An ~5-fold increase in GC phenotype B cells (B220$^+$Fas$^+$) **(b**, right panel**)** and 20-fold increase in CD11b$^+$ cells **(c)** was detected in spleen of B6-Qa-1(D227K) mice upon LCMV-Armstrong infection compared to B6-(Qa-1^{WT}) mice. **(d)** 6-8 week old WT B6 and D227K mice were infected i.p. with 10^6 PFU LCMV-Armstrong. At day 8, mice were reinfected i.p. with 10^5 PFU LCMV-Armstrong. 28 days after primary infection, serum from LCMV-infected WT B6 and D227K mice was analyzed for the production of antibodies specific for dsDNA. Data represent mean ± SEM. (3-6 mice/group)

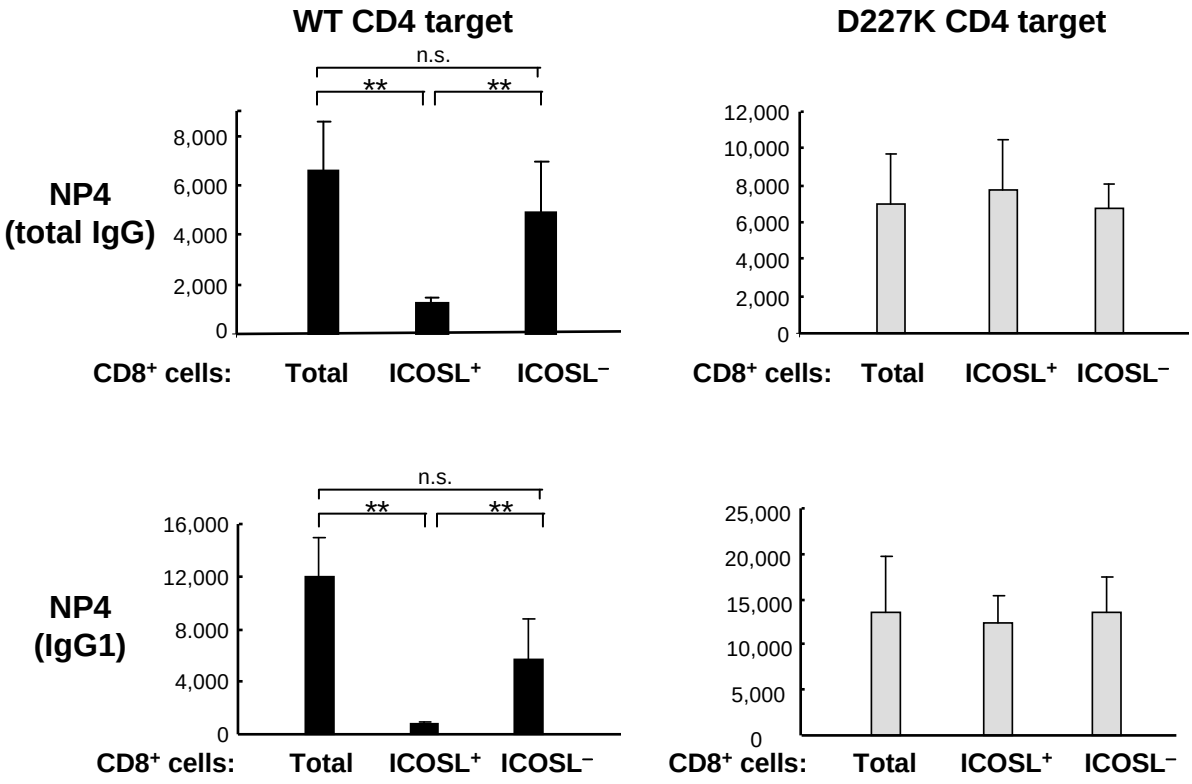

Supplementary Figure 4. Suppression of high affinity Ab response by ICOSL$^+$ CD8 cells, but not by total CD8 or ICOSL$^-$ CD8 cells:

Rag2$^{-/-}$ mice were transferred with 2×10^6 naïve WT B cells along with 1×10^6 naïve WT or B6-Qa-1 D227K CD4 cells. In addition, *Rag2*$^{-/-}$ mice were given either unseparated CD8 cells or ICOSL$^+$ enriched and ICOSL$^-$ CD8 cells from KLH/CFA-immunized mice. Immediately after cell transfer, *Rag2*$^{-/-}$ mice were immunized i.p. with 100 μg NP_{19}-KLH in CFA. Mice were reimmunized i.p. with 50 μg NP19-KLH in IFA and the NP specific Ab response was measured by ELISA.

Qa-1 expression on B cells

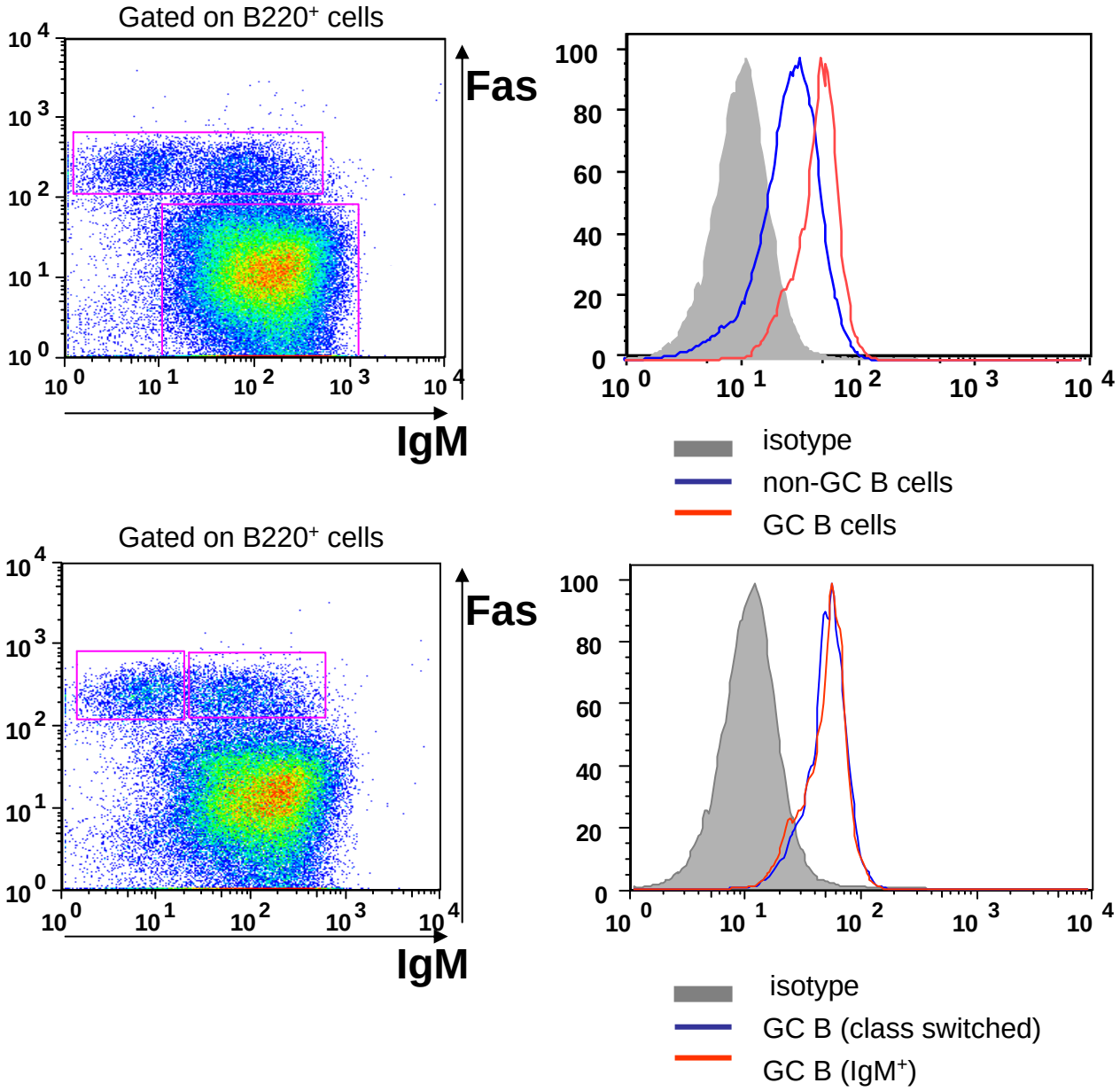

Supplementary Figure 5. **Expression of Qa-1 by naïve and GC B cells**.

WT B6 mice were immunized with 100 μg KLH in CFA. Seven days after immunization, splenic B cells were analyzed for Qa-1 expression. Levels of Qa-1 expression on naïve and activated B cells (GC B cells) were analyzed (**upper panel**). Levels of Qa-1 expression by class-switched and IgM$^+$ GC B cell were compared (**lower panel**) .

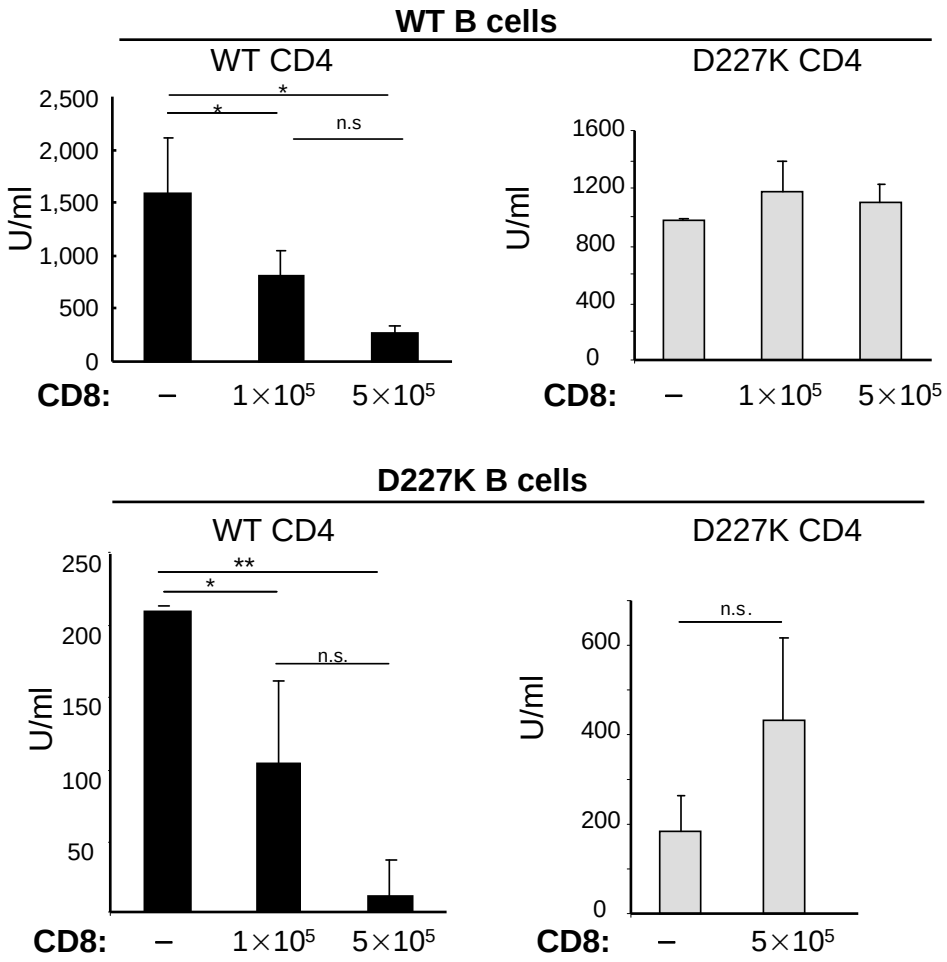

Supplementary Figure 6. Ab response after transfer of B cells, CD4 cells and CD8 cells into *Rag2*$^{-/-}$ mice.

2×10^6 naïve B cells from 2 month old B6.Qa-1 WT (upper panel) or B6.Qa-1(D227K) mice (lower panel) were transferred along with 1×10^6 CD25$^+$ depleted CD4 cells from B6.Qa-1(WT) or B6.Qa-1(D227K) mice. Titrated numbers of CD44$^+$ CD8 cells isolated from KLH/CFA-immunized mice were given to *Rag2*$^{-/-}$ mice. Immediately after transfer, *Rag2*$^{-/-}$ recipients were immunized i.p. with 100 μg KLH in CFA. At day 10, mice were reimmunized i.p. with 50 μg KLH in IFA. At day 17, NP-specific Ab responses were measured by ELISA, as summarized below:

B cells	CD4 cells	Suppression
WT	WT	+++
WT	D227K	–
D227K	WT	+++
D227K	D227K	–

Target cells of Qa-1-restricted suppression

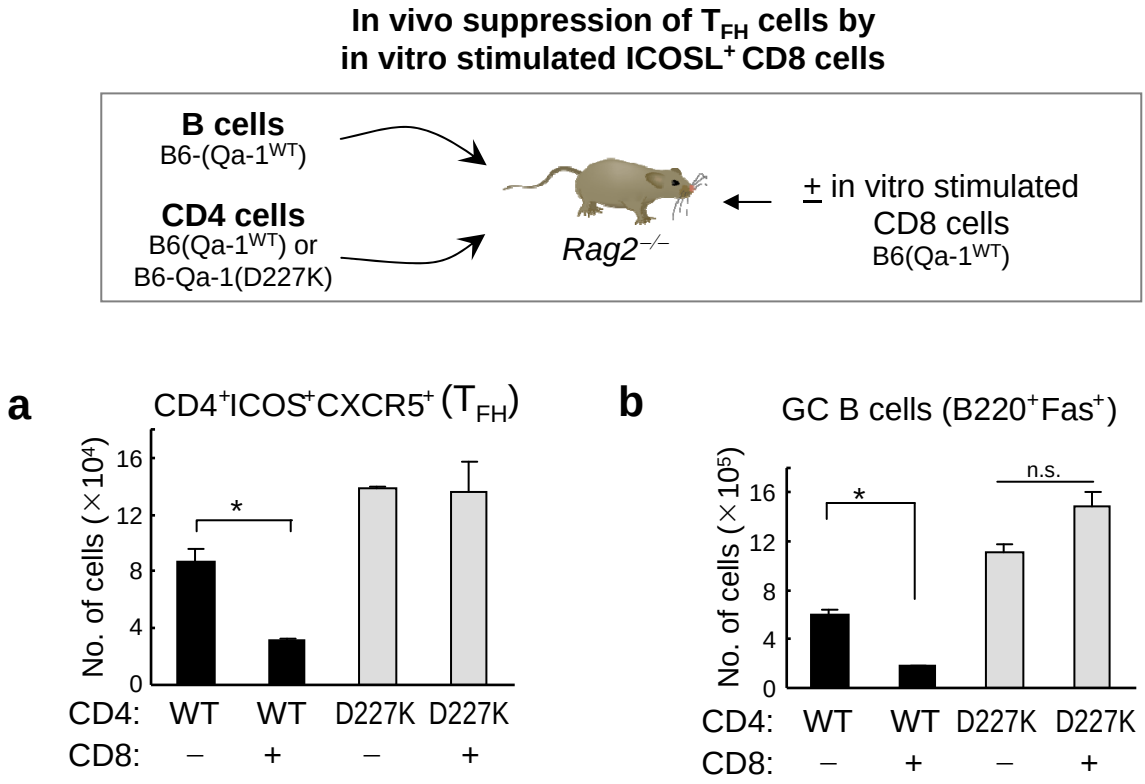

Supplementary Figure 7. Suppression of T_{FH} cells by in vitro stimulated ICOSL$^+$ CD8 cells.

Rag2$^{-/-}$ mice were given 2×10^6 naïve B cells from WT mice and 10^6 CD4 cells from either B6.Qa-1(WT) or B6.Qa-1(D227K) mice. After injection of 2×10^5 in vitro-stimulated ICOSL$^+$ CD8$^+$ cells into each *Rag2*$^{-/-}$ recipient, mice were immunized i.p. with 100 μg NP_{19}-KLH in CFA and reimmunized i.p. with 50 μg NP_{19}-KLH in IFA at day 12. Spleen cells from different groups of *Rag2*$^{-/-}$ hosts were analyzed for levels of **a**) follicular helper T cells (CD4$^+$ICOS$^+$CXCR5$^+$) and **b**) GC B cells (B220$^+$Fas$^+$) by FACS at day 28 after primary immunization. Mean cellularity ± SEM is shown (n=3-5/group).

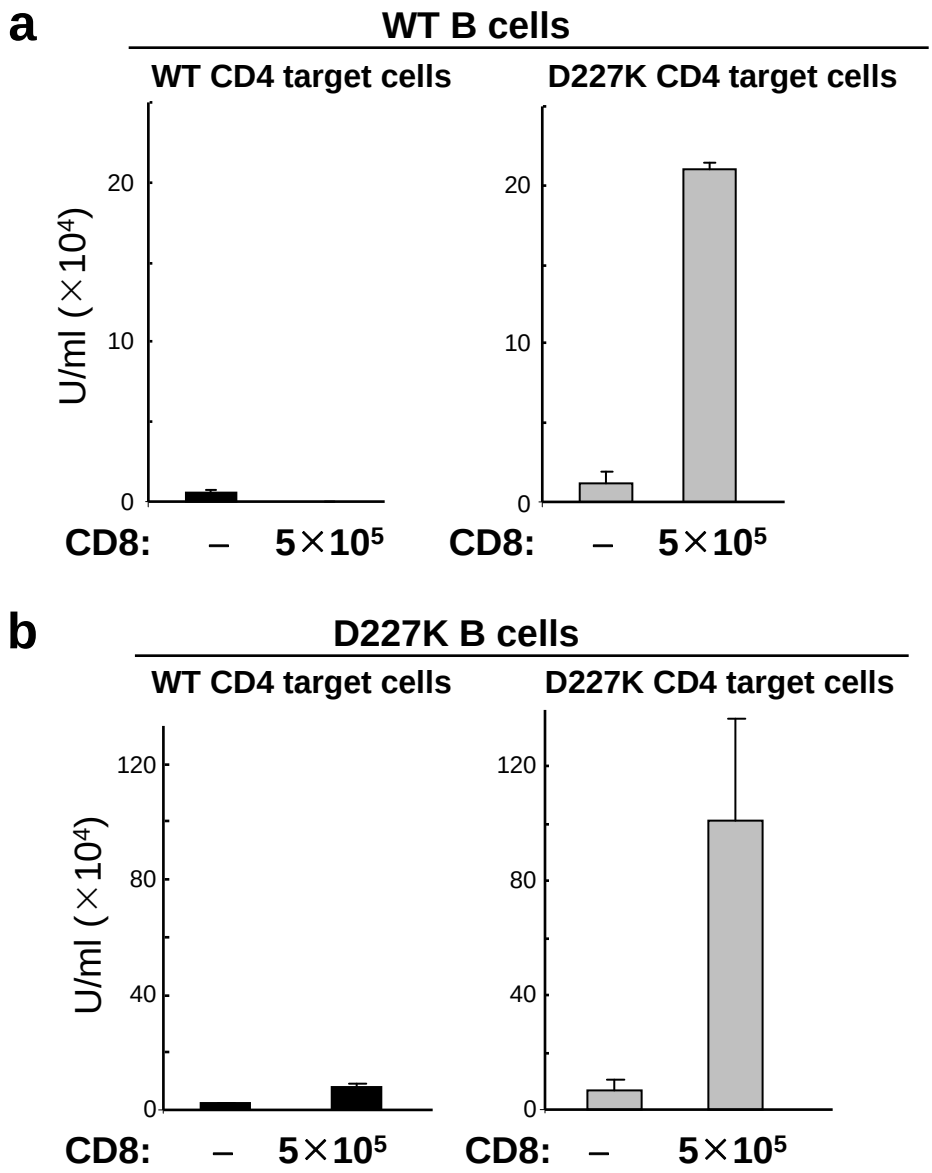

Supplementary Figure 8. Autoantibody generation after transfer of B, CD4 and CD8 cells into *Rag2*$^{-/-}$ *hosts*.

2×10^6 naïve B cells from 2 month old B6.Qa-1(WT) mice (**a**) and B6.Qa-1(D227K) mice (**b**) were transferred along with 10^6 $CD25^+$ depleted CD4 T cells from WT or D227K mice. 5×10^5 $CD44^+$ CD8 cells isolated from KLH/CFA-immunized mice were transferred into *Rag2*$^{-/-}$ hosts. Immediately after transfer, mice were immunized i.p. with 100 μg KLH in CFA. At day 10, mice were reimmunized i.p. with 50 μg KLH in IFA. At day 21, anti-dsDNA Ab was measured by ELISA.

Cytokine production by in vitro generated T_H sublineages

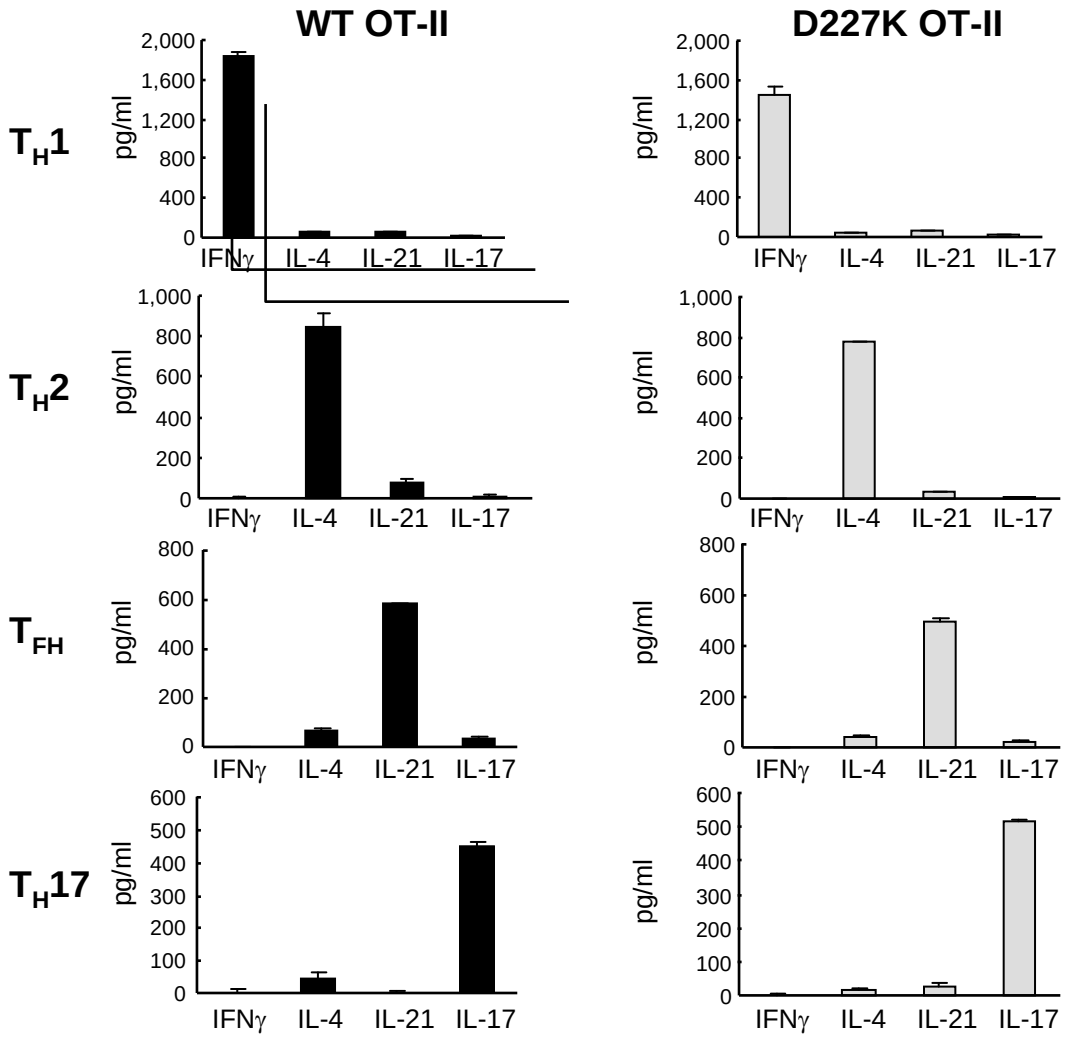

Supplementary Figure 9. T_H lineage differentiation in vitro: Cytokine profiles.
T_H1: 5 ng/ml rmIL-12 and 10 μg/ml anti-IL-4 Ab, T_H2: 10 ng/ml rmIL-4 Ab, 10 μg/ml anti-IL-12 Ab, 10 μg/ml anti-IFNγ Ab, T_{FH}: 50 ng/ml IL-21, 10 μg/ml anti-IL-4 Ab, 10 μg/ml IFNγ Ab, 20 μg/ml anti-TGFβ Ab and 20 ng/ml rmIL-6, T_H17: 3 ng/ml TGFβ, 20 ng/ml rIL-6, 20 ng/ml rIL-23, 10 μg/ml anti-IL-4 Ab, 10 μg/ml anti-IFNγ Ab, 10 μg/ml anti-IL-12 Ab. At day 5, cells were harvested and 10^5 cells were restimulated with 0.5 μg/ml OT-II peptide for 24h. Cell supernatants were subjected to cytokine analysis by ELISA.

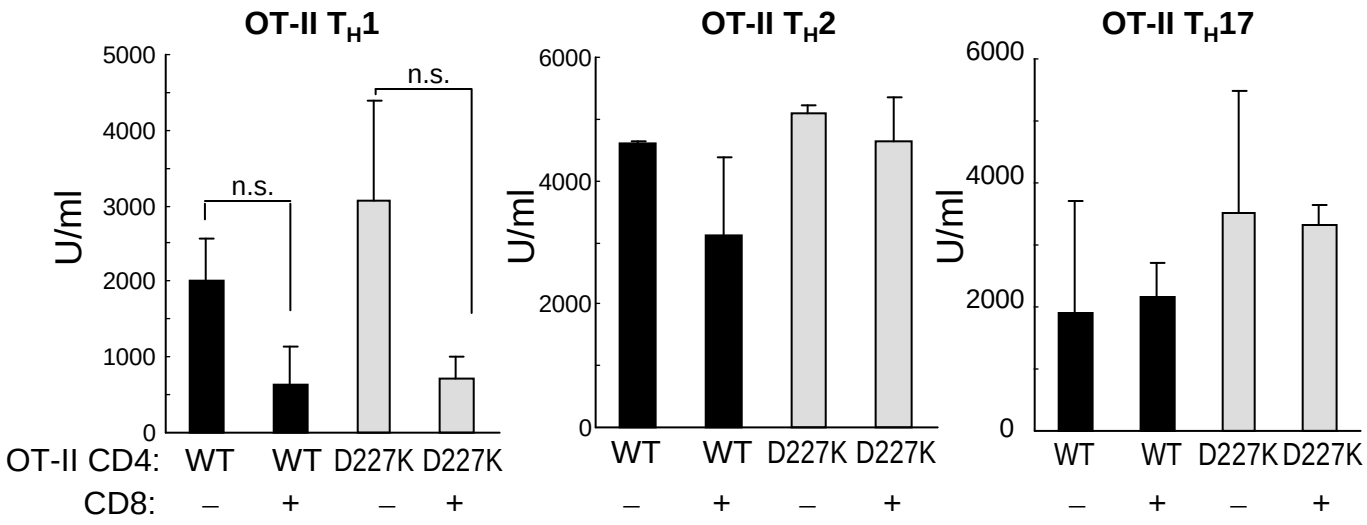

Supplementary Figure 10. Transfer of in vitro differentiated T_H sublineages and Ab response.

Naïve OT-II cells were differentiated into T_H1, T_H2 and T_H17 cells using following protocol: 1 μg/ml OT-II peptide was used. T_H1: 5 ng/ml rmIL-12 and 10 μg/ml anti-IL4 Ab, T_H2: 10 ng/ml rmIL-4 Ab, 10 μg/ml anti-IL-12 Ab, 10 μg/ml anti-IFNγ Ab, T_{FH}: 50 ng/ml IL-21, 10 μg/ml anti-IL-4 Ab, 10 μg/ml anti-IFNγ Ab, 20 μg/ml anti-TGFβ Ab and 20 ng/ml rmIL-6, T_H17: 3 ng/ml TGFβ, 20 ng/ml rIL-6, 20 ng/ml rIL-23, 10 μg/ml anti-IL-4 Ab, 10 μg/ml anti-IFNγ Ab, 10 μg/ml anti-IL-12 Ab. At day 5, cells were harvested and 1×10^5 cells were transferred into *Rag2*$^{-/-}$ recipients along with 2×10^6 WT naïve B cells and 2×10^5 sorted CD44$^+$ CD8 cells from KLH/CFA-immunized B6 donors. Immediately after transfer, *Rag2*$^{-/-}$ mice were immunized i.p. with 100 μg/ml NP_{13}-OVA in CFA. 15 days later, NP_{23} binding IgG1 responses were measured by ELISA.

Mechanism of Qa-1-restricted suppression: Contribution of perforin to Qa-1-restricted inhibition

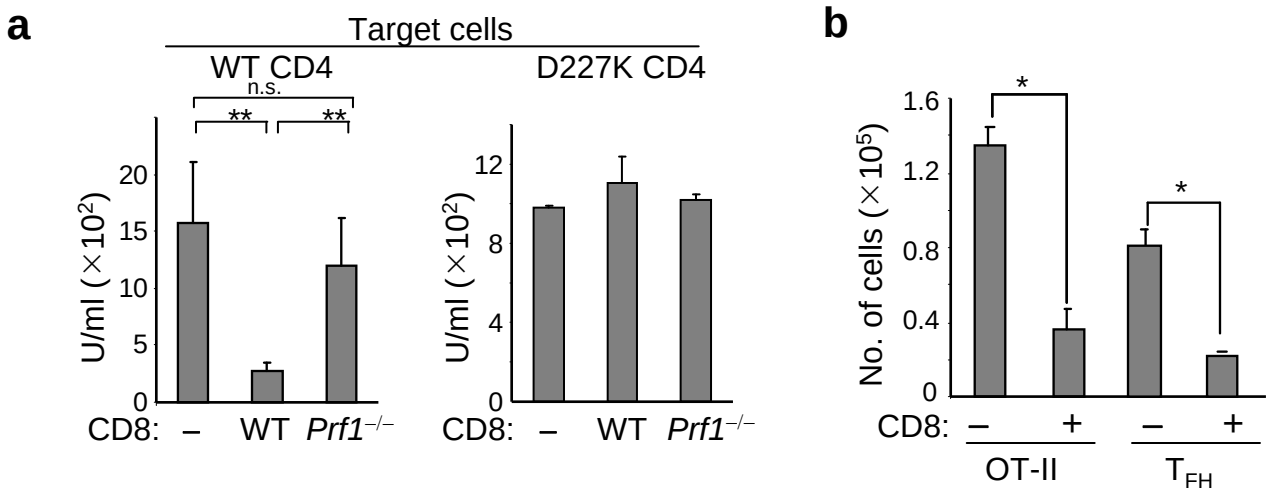

Supplementary Figure 11. **Perforin dependent suppression of T_{FH} by CD8 Treg**:
Ab response after transfer of B, CD4 and CD8 cells into *Rag2*$^{-/-}$ mice. 2×10^6 WT naïve B cells were transferred along with 1×10^6 $CD25^+$ depleted CD4 cells from B6.Qa-1(WT) or B6.Qa-1(D227K) mice into *Rag2*$^{-/-}$ hosts. $CD44^+$ cells isolated from KLH/CFA immunized WT or *Prf1*$^{-/-}$ mice were transferred into *Rag2*$^{-/-}$ hosts. Immediately after cell transfer, *Rag2*$^{-/-}$ recipients were immunized i.p. with 100 μg NP_{19}-KLH in CFA. At day 10, mice were reimmunized i.p. with 50 μg NP_{19}-KLH in IFA and NP specific Ab responses were measured by ELISA seven days later (**a**). (**b**) Enumeration of OT-II and T_{FH} cells in *Rag2*$^{-/-}$ $\gamma c^{-/-}$ recipients: Naïve WT OT-II (5×10^5) were transferred along with CD8 cells (7×10^5) from immune donors into *Rag2*$^{-/-}\gamma c^{-/-}$ mice, followed by immunization with 100 μg NP_{13}-OVA in CFA and boosting with 50 μg NP13-OVA in IFA at day 10. On day 18, the numbers of OT-II cells ($V_\beta5^+CD4^+$) and OT-II cells with a T_{FH} phenotype ($ICOS^+CD200^+CD4^+$) in spleen were enumerated by FACS analysis.

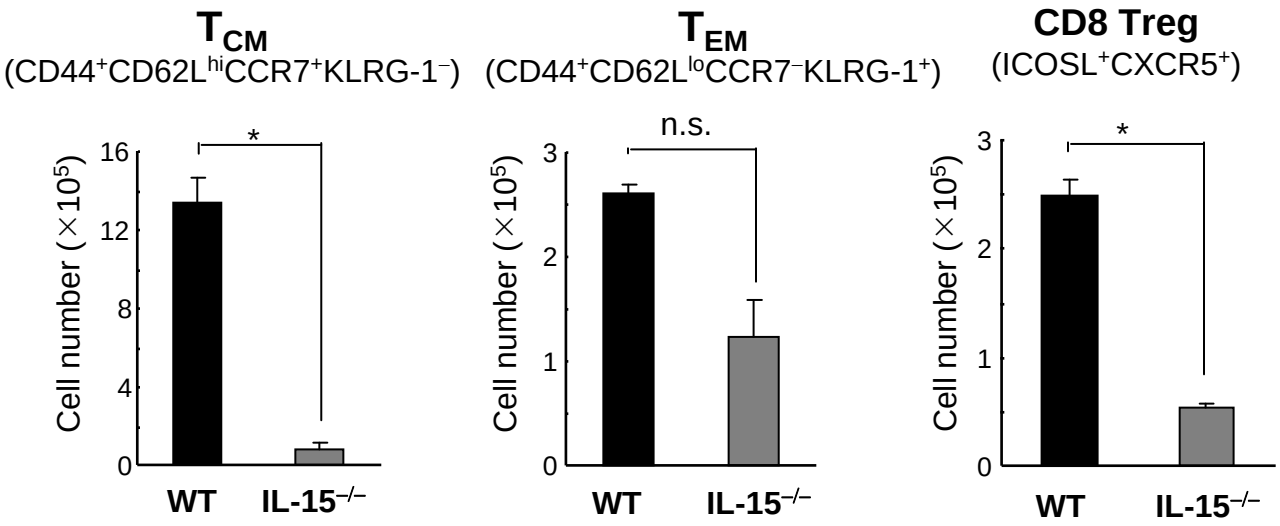

Supplementary Figure 12. Memory and regulatory CD8 T cells in WT and IL-15$^{-/-}$ mice: WT B6 and IL-15$^{-/-}$ mice were immunized i.p. with 100 μg KLH/CFA. 38 days later, the number of CD8 memory subsets and ICOSL^{+}CXCR5^{+} CD8 cells was analyzed by FACS. Central memory (T_{CM}) and effector memory (T_{EM}) CD8 cells were defined according to differential expression of CD44, CD62L, CCR7 and KLRG-1.

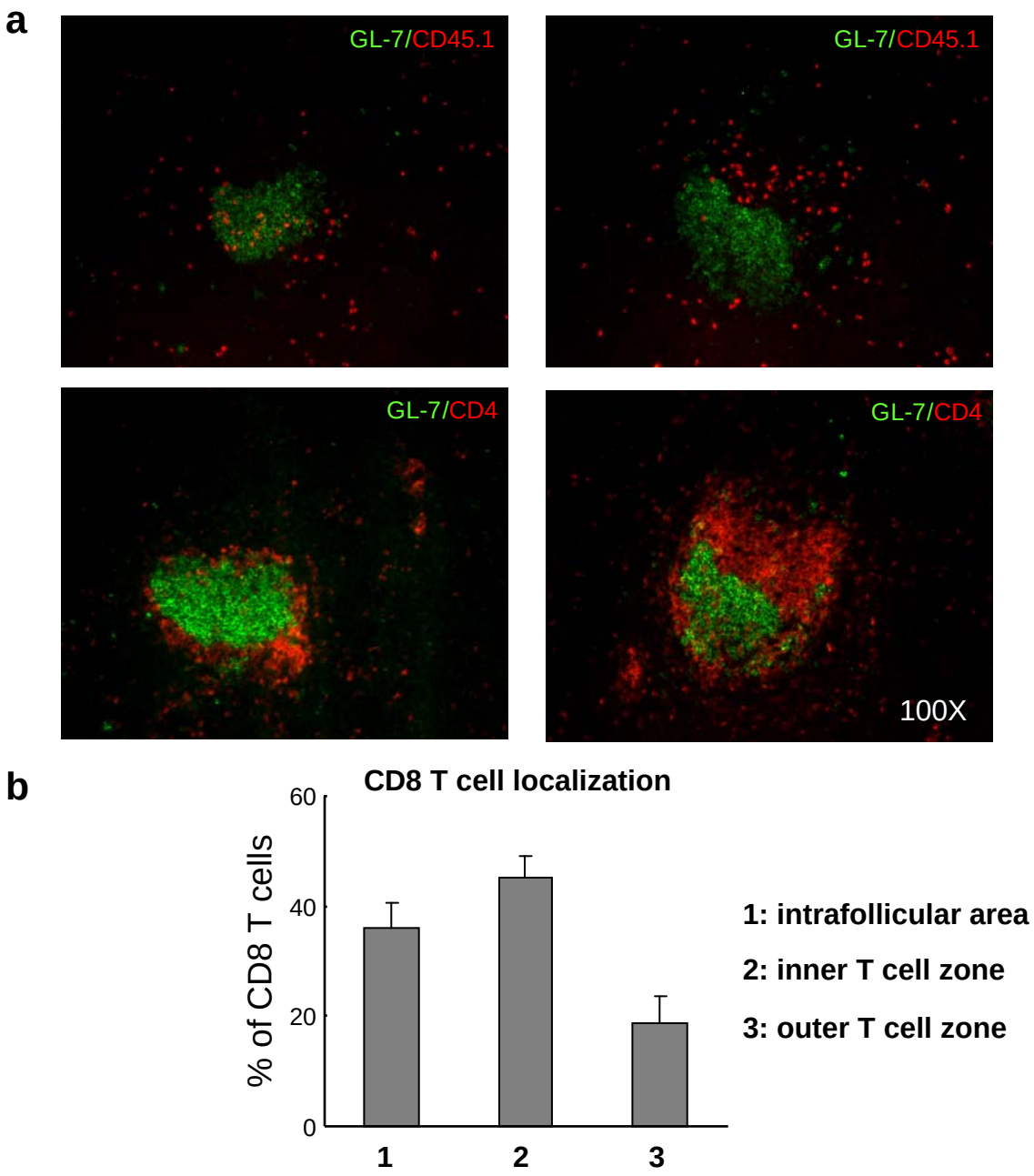

Supplementary Figure 13. Follicular localization of CD8 cells:
Rag2$^{-/-}$ mice were transferred with 3×10^6 WT B cells and 2×10^6 WT CD4 cells. Mice were immunized with 100 μg NP_{19}-KLH. At day 10 post immunization, 1×10^6 sorted CD44$^+$ CD8 cells isolated from KLH/CFA-immunized CD45.1 syngeneic mice were transferred into *Rag2*$^{-/-}$ hosts. Spleens from these mice were harvested at day 5. Localization of GC B cells, CD4 cells and CD8 cells was analyzed by staining spleen tissue sections with GL-7 and anti-CD45.1 or GL-7 and anti-CD4 Abs (**a**). The percent of CD8 cells that migrated into B and T cell zones was quantified by counting cells within the GL-7$^+$ area, the inner CD4 T cell area and outer CD4 T cell zone. The inner T cell zone was defined by the area with sporadic distribution of B cells. Outer T cell area was defined by the outer layer of the CD4$^+$ T cell zone with no B cells (**b**).

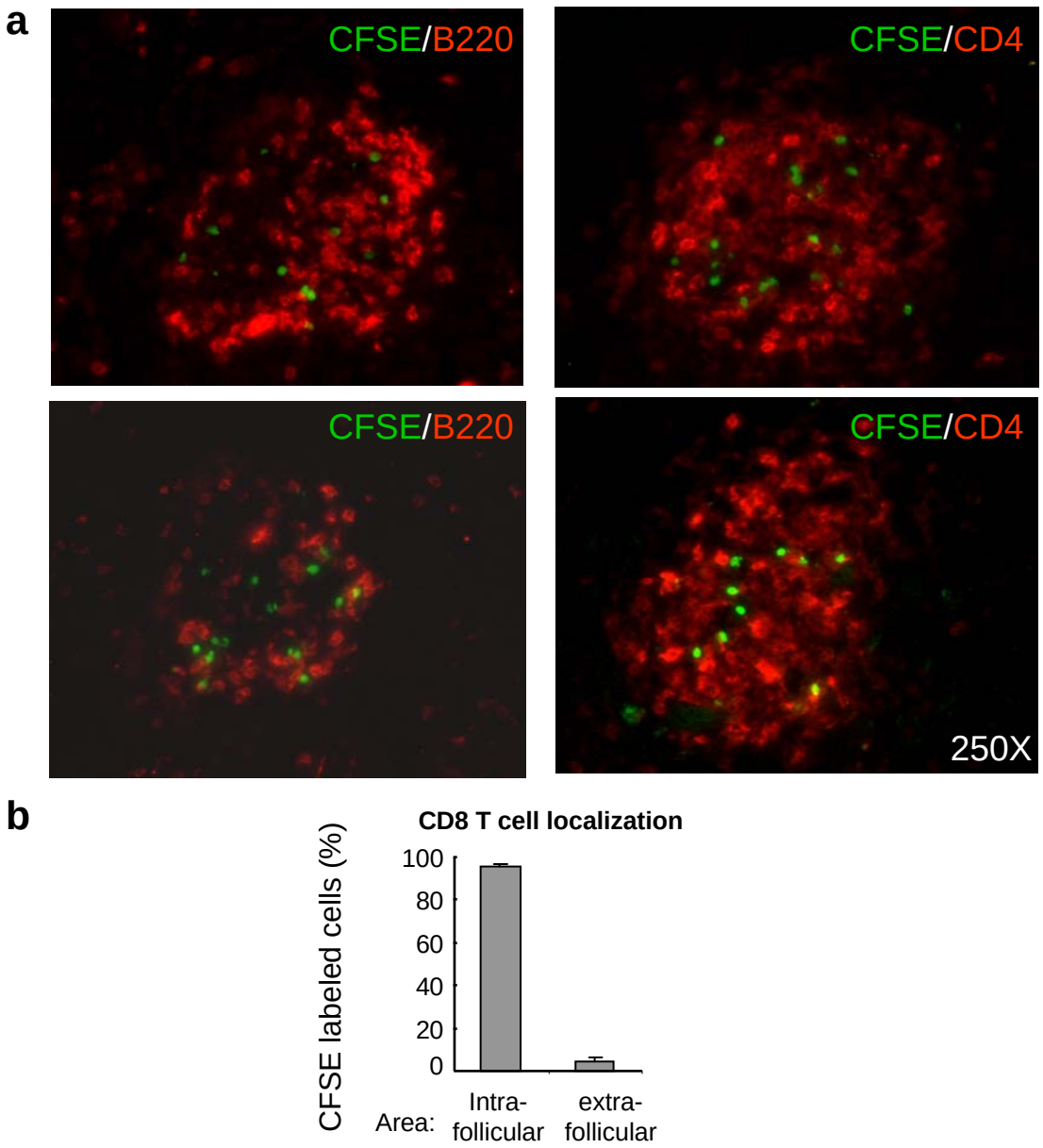

Supplementary Figure 14. Follicular localization of CD8 cells:
Rag2$^{-/-}$ mice were transferred with 3×10^6 WT B cells and 2×10^6 WT CD4 cells before immunization with 100 mg NP19-KLH. Three days later, 0.5×10^6 sorted CXCR5$^+$ CD8 cells (>99%pure) from KLH/CFA-immunized mice were CFSE labeled before transfer into *Rag2*$^{-/-}$ hosts and harvesting 24h later. Localization of B cells and CD4 cells in splenic tissue sections was determined using anti-B220 and anti-CD4 antibodies. Localization of CXCR5$^+$ CD8 cells was detected by green fluorescence (CFSE). Two independent follicles in consecutive sections are shown (**a**). Quantification of CD8 cells within or outside of follicular areas is shown (20 different follicles were analyzed) (**b**).

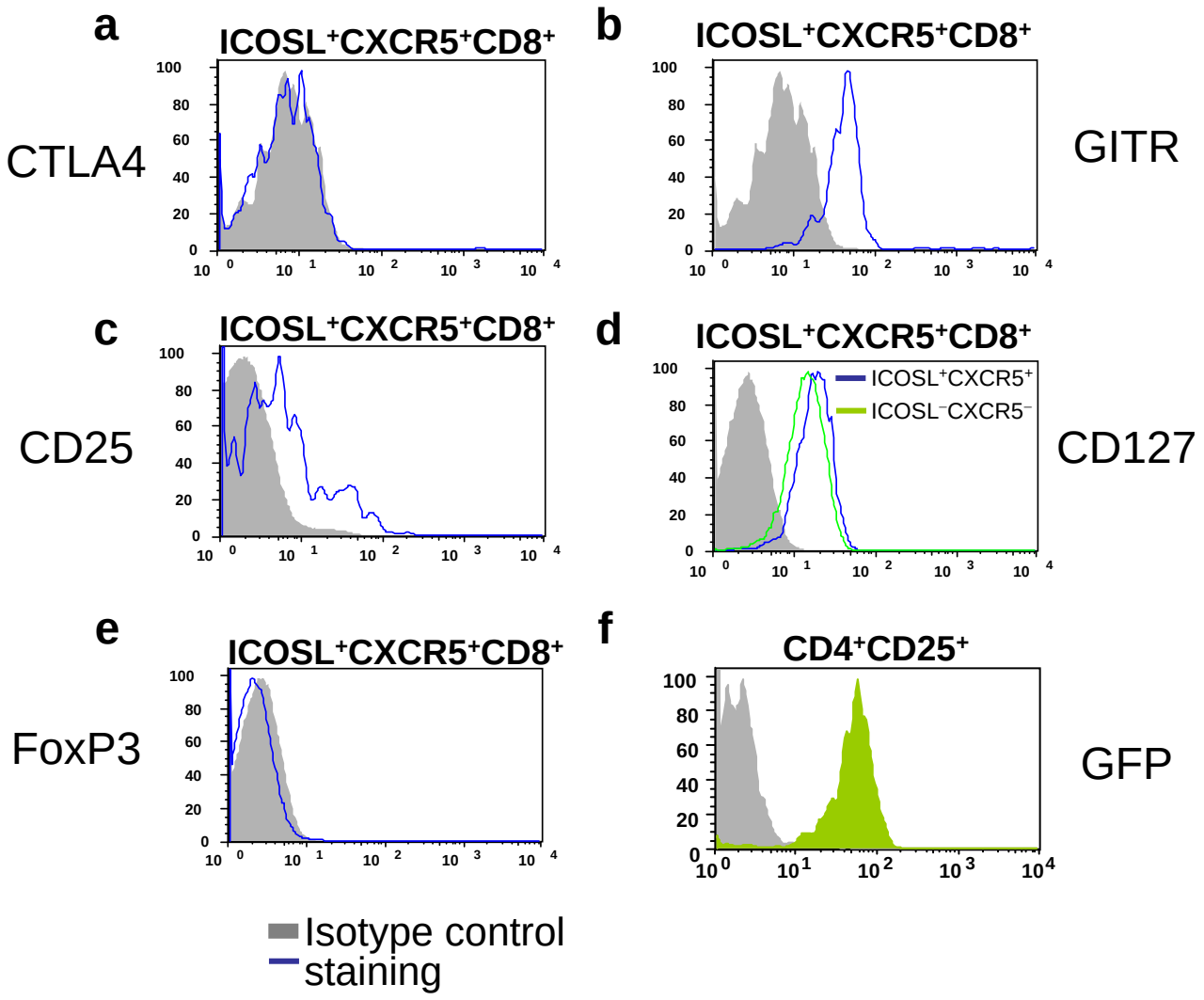

Supplementary Figure 15. Analysis of expression of canonical CD4 Treg markers. ICOSL$^+$CXCR5$^+$ CD8 T cells from B6 mice one week after immunization with 100 μg KLH/CFA were examined for expression of CTLA-4 (**a**), GITR (**b**), CD25 (**c**) and IL-7Rα (CD127) (**d**) using appropriate antibodies and isotype controls. ICOSL$^+$CXCR5$^+$ CD8 T cells from FoxP3-GFP knockin mice (immunized with 100 μg KLH/ CFA i.p. as above) were also examined for FoxP3 by measuring GFP expression (**e**). The level of GFP expression by CD4$^+$CD25$^+$ cells from FoxP3-GFP mice (positive control) is shown by comparing with CD4$^+$CD25$^-$ cells (negative control) (**f**). Groups a-e are gated on ICOSL$^+$CXCR5$^+$ CD8 cells. The level of CD127 expression by ICOSL$^+$CXCR5$^+$ CD8 cells was compared to ICOSL$^-$CXCR5$^-$ cells (d).

Phenotype of in vitro differentiated OT-II T_{FH} cell
(no IL-6 supplementation)

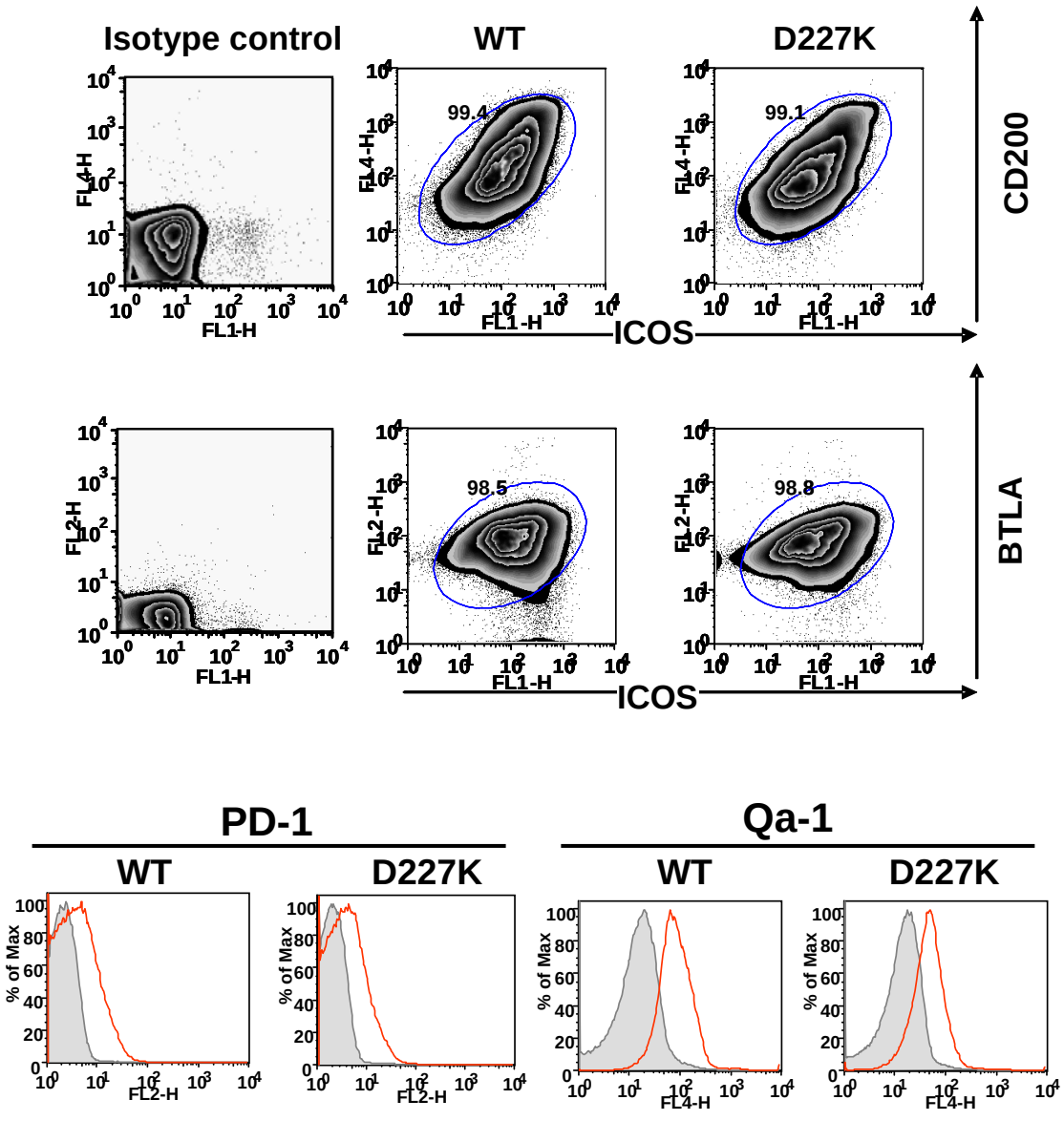

Supplementary Figure 16. Phenotype of OT-II cells confirmed under T_{FH} conditions. Naïve OT-II cells ($CD44^{-}CD62L^{hi}$) from WT and D227K mice were stimulated with 1 μg/ml OT-II peptide, 50 ng/ml IL-21, 10 μg/ml anti-IFNγ, 10 μg/ml anti-IL-4 and 20 μg/ml anti-TGFβ Abs for 5 days. Surface expression of ICOS, OX2 (CD200), BTLA, PD-1 and Qa-1 was analyzed by FACS.

Phenotype of in vitro differentiated OT-II T_{FH} cells
(with IL-6 supplementation)

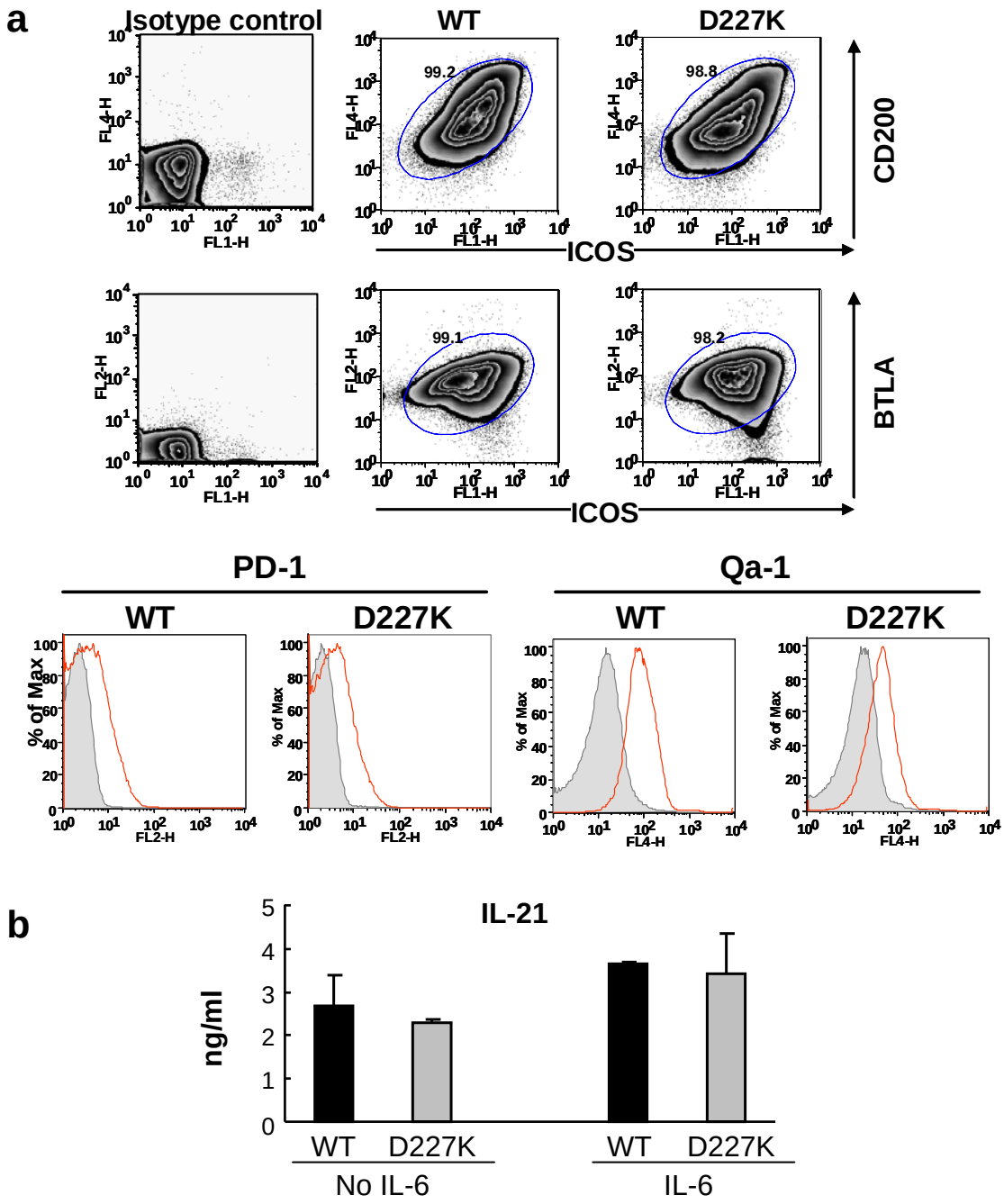

Supplementary Figure 17. Phenotype of OT-II cells confirmed under T_{FH} conditions.
a) Naïve OT-II cells ($CD44^{-}CD62L^{hi}$) from WT and D227K mice were stimulated with 1 μg/ml OT-II peptide, 50 ng/ml IL-21, 20 ng/ml IL-6, 10 μg/ml anti-IFNγ, 10 μg/ml anti-IL-4 and 20 μg/ml anti-TGFβ Abs for 5 days. Surface expression of ICOS, OX2 (CD200), BTLA, PD-1 and Qa-1 was analyzed by FACS. **b**) At day 5, cells were harvested and 1×10^5 cells were restimulated with 1 μg/ml anti-CD3 Ab for 24 hrs. Production of IL-21 was compared in T_{FH} culture in the presence or absence of IL-6. IL-6 supplementation did not affect the surface phenotype or IL-21 cytokine response of OT-II T_{FH} cells.